Supplementary Information

Promoting nickel oxidation state transformation in NiFe hydroxide nanosheets for efficient oxygen evolution reaction

Wenwen Peng,[a] Xueqiu Qin,[a] Xiaocan Mo,[a] Jinrui Zhao,[a] Shuhan Li,[a] Guanfang Liang,[a] Tong Chen,[a] Jiaao Wei,[a] Shuifeng Zhang*[b], Xiaokun Li*[a], Youlin Zhang,*[a] and Wei Chen*[a]

[a]*School of Chemistry and Pharmaceutical Sciences, Guangxi Normal University, Guilin 541004, China*

[b]*Library, Guangxi Normal University, Guilin 541004, P.R. China*

*Corresponding authors:

Shuifeng Zhang (sfzhang@gxnu.edu.cn);

Xiaokun Li (lixk@mailbox.gxnu.edu.cn);

Youlin Zhang (zhangyl0109@mailbox.gxnu.edu.cn);

Wei Chen (weichen@gxnu.edu.cn)

1. Experimeental Details

1.1 Materials and Reagents

Nickel nitrate ($Ni(NO_3)_2·6H_2O$, Xilong, 98.0%), iron(II) sulfate heptahydrate ($FeSO_4·7H_2O$, Aladdin, 99.0%), N-2-hydroxyethylpiperazine-N'-2-ethanesulfonic acid (HEPES, Aladdin, 99.0%), sodium hydroxide (NaOH, Xilong, 96.0%), and isopropanol (Xilong, 99.7%). All chemicals were used as received without further purification, and all solutions were prepared with ultrapure water (18.2 MΩ cm^{-1}).

1.2 Preparation of HEPES (H) Buffer Solution

1.1915 g of HEPES powder was weighed and dissolved in 80 mL of ultrapure water. Using 1 M NaOH solution as the pH adjustor, the pH value of the solution was calibrated to 8.5 with a pH meter, and the final volume was fixed at 100 mL, resulting in a final concentration of 50 mM for H. The prepared solution was stored at room temperature for subsequent use. The H buffer solutions with other pH values were prepared following the identical procedure.

1.3 Synthesis of NiFe(III) hydroxide

2.5 mL of 8 mM $Ni(NO_3)_2$ solution was mixed with 5 mL of 50 mM HEPES buffer (pH 8.5). After 5 minutes, 2.5 mL of 2 mM $Fe_2(SO_4)_3$ solution was added to the mixture. The solution rapidly turned to brownish-yellow, accompanied by the formation of a brownish-yellow precipitate. Subsequently, the product was collected via centrifugation, and finally subjected to freeze-drying to obtain the NiFe(III) hydroxide sample.

1.4 Synthesis of other control samples

Synthesis of Fe hydroxide: 5 mL of the 2 mM $FeSO_4$ solution was mixed with 5 mL of 50 mM HEPES buffer. The solution rapidly changes from gray-green to reddish-brown, accompanied by the formation of reddish-brown flocculent material. After a period of time, the reddish-brown flocculent material settles to the bottom. The reddish-brown precipitate was then centrifuged, washed for three times with ethanol and water, and finally freeze-dried to obtain the Fe hydroxide sample.

Synthesis of Ni hydroxide: 5 mL of the 4 mM $Ni(NO_3)_2$ solution was mixed with 5 mL of 50 mM HEPES buffer. The solution exhibits no color change. Finally, the mixture

was freeze-dried to obtain the Ni hydroxide sample.

Synthesis of NiFe hydroxide (no H)： Without H, 5 mL of 4 mM $Ni(NO_3)_2$ was mixed with 5 mL of 2 mM $FeSO_4$. The solution exhibits no color change. Then, the sample was freeze-dried.

1.5 Structural characterizations

The powder X-ray diffraction (XRD) was carried out by a D8 ADVANCE (BRUKER Germany) with Cu-Kα radiation (λ = 1.54 Å), and operated at 45 kV, 40 mA and on a diffracted-beam graphite monochromator in scanning mode (step = 0.01313° 2θ).Transmission Electron Microscopy (TEM, Talos F200S) was used to analyze the structure and morphology of the samples. Scanning TEM (STEM) was used for atomic resolution analysis microscopy. X-ray photoelectron spectroscopy (XPS) experiments were carried out on a VG scientific ESCALAB 2201XL instrument using Al-Kα X-rays. Inductively Coupled Plasma Optical Emission Spectrometer(ICP-OES) was used for the quantitative analysis of the metallic elements in the samples..The Raman spectrometer model is InVia Qontor, the laser is 785 nm, and the wavelength range is 200 ~ 800 cm^{-1}.

1.6 *In situ* Raman measurements:

The *in situ* Raman measurements were performed using the Raman microscope and selfcustomed cell (Teflon material with a quartz window positioned between the sample and the objective). The working electrode was immersed in the electrolyte through the cell wall, and the electrode plane was maintained perpendicular to the laser. A carbon rod and Hg/HgO electrodes were used as counter electrodes and reference electrodes, respectively. The current was measured over time in a 1.0 M KOH solution over a potential range from 1.2 to 1.7 V (vs. RHE).

2. Supplementary Figures and Tables

Fig. S1 Photo of the synthesized NiFe hydroxide sample.

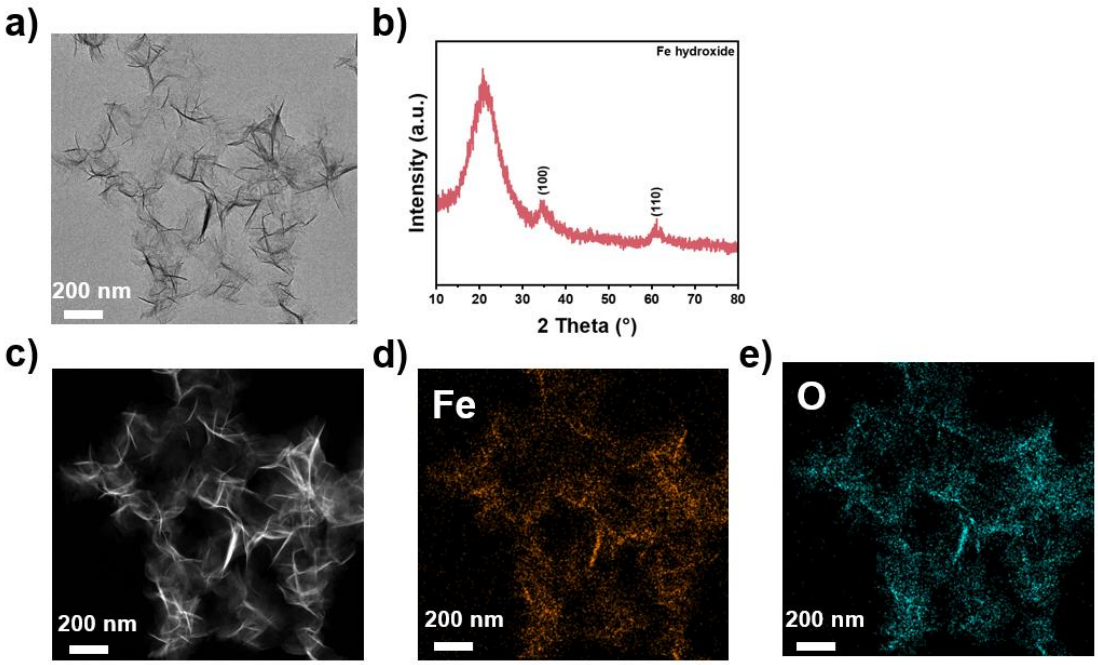

Fig. S2 Characterizations of the Fe hydroxide nanosheets. (a) TEM image, (b) XRD spectrum and (c-e) EDS-mapping images.

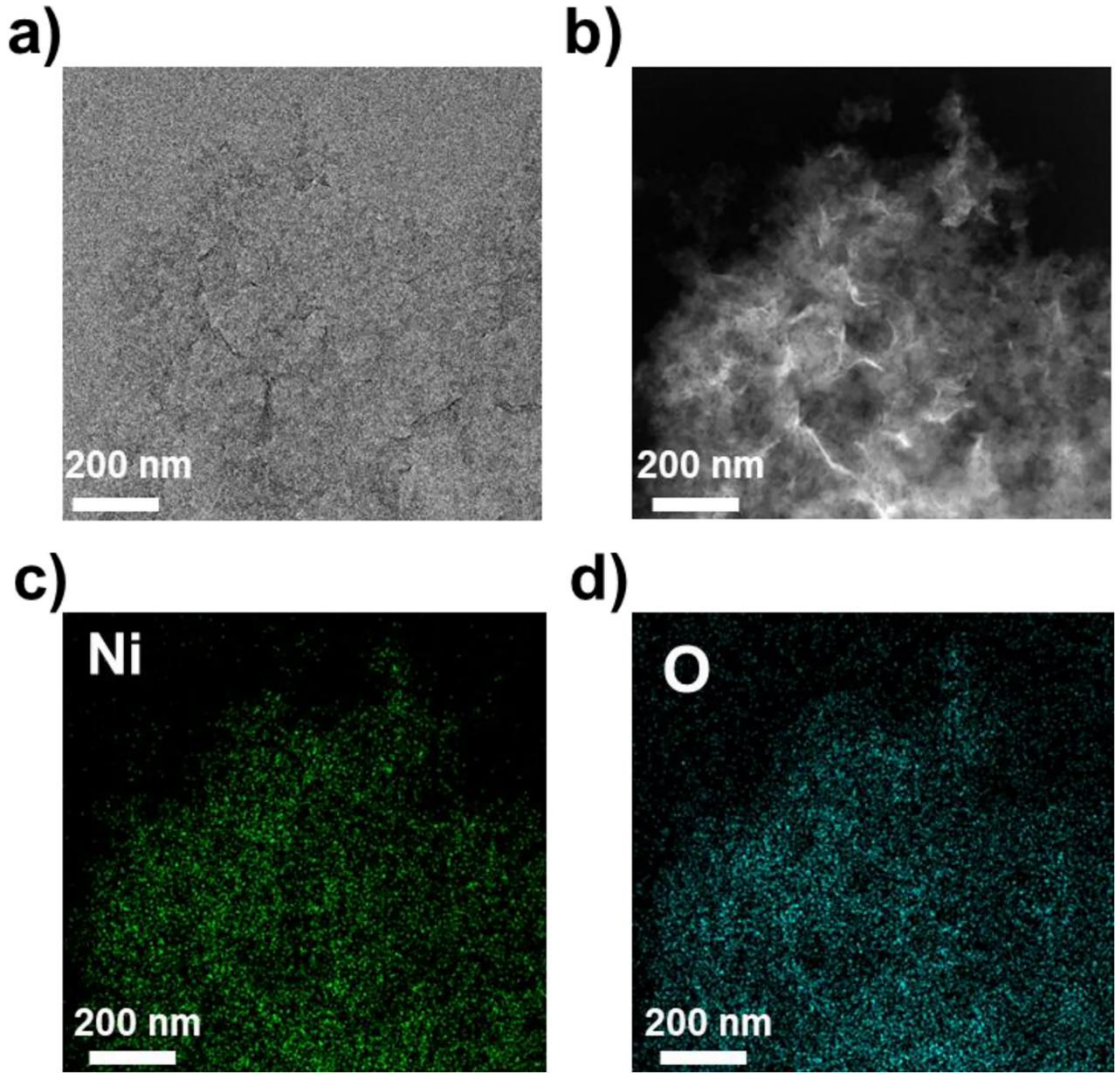

Fig. S3 Characterizations of the Ni hydroxide nanosheets. (a) TEM image, (b-d) EDS-mapping images of the Ni hydroxide nanosheets.

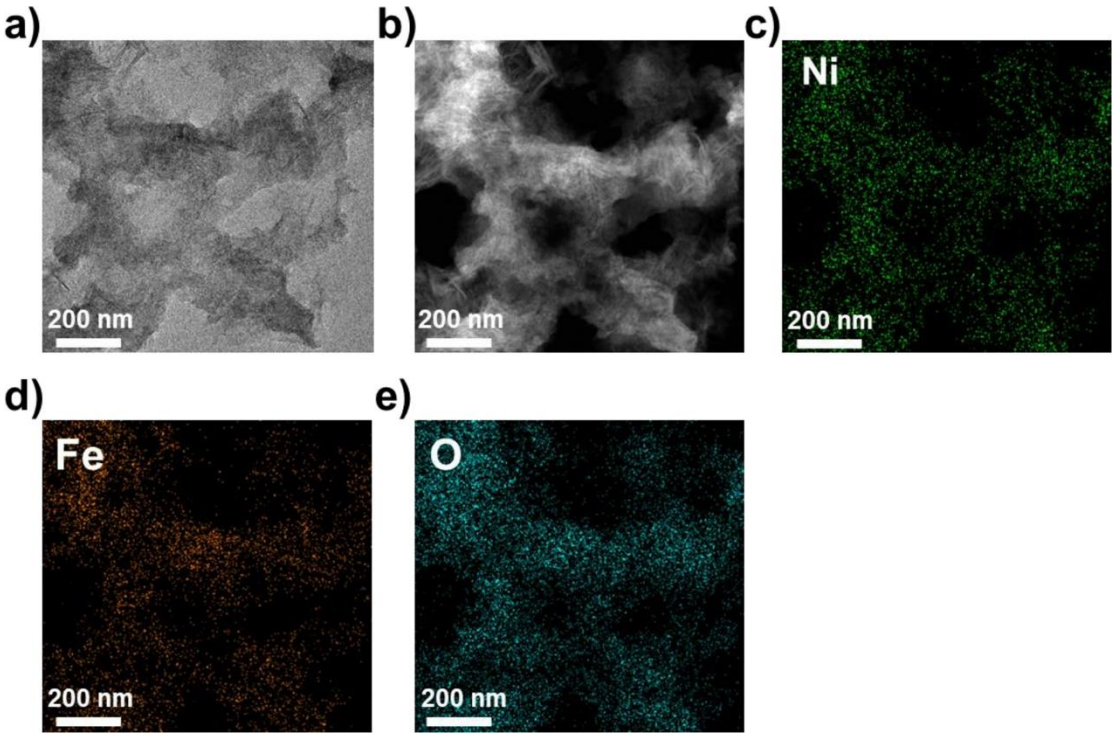

Fig. S4 Characterizations of the NiFe hydroxide nanosheets (no H). (a) TEM image, (b-d) EDS-mapping images of the NiFe hydroxide nanosheets (no H).

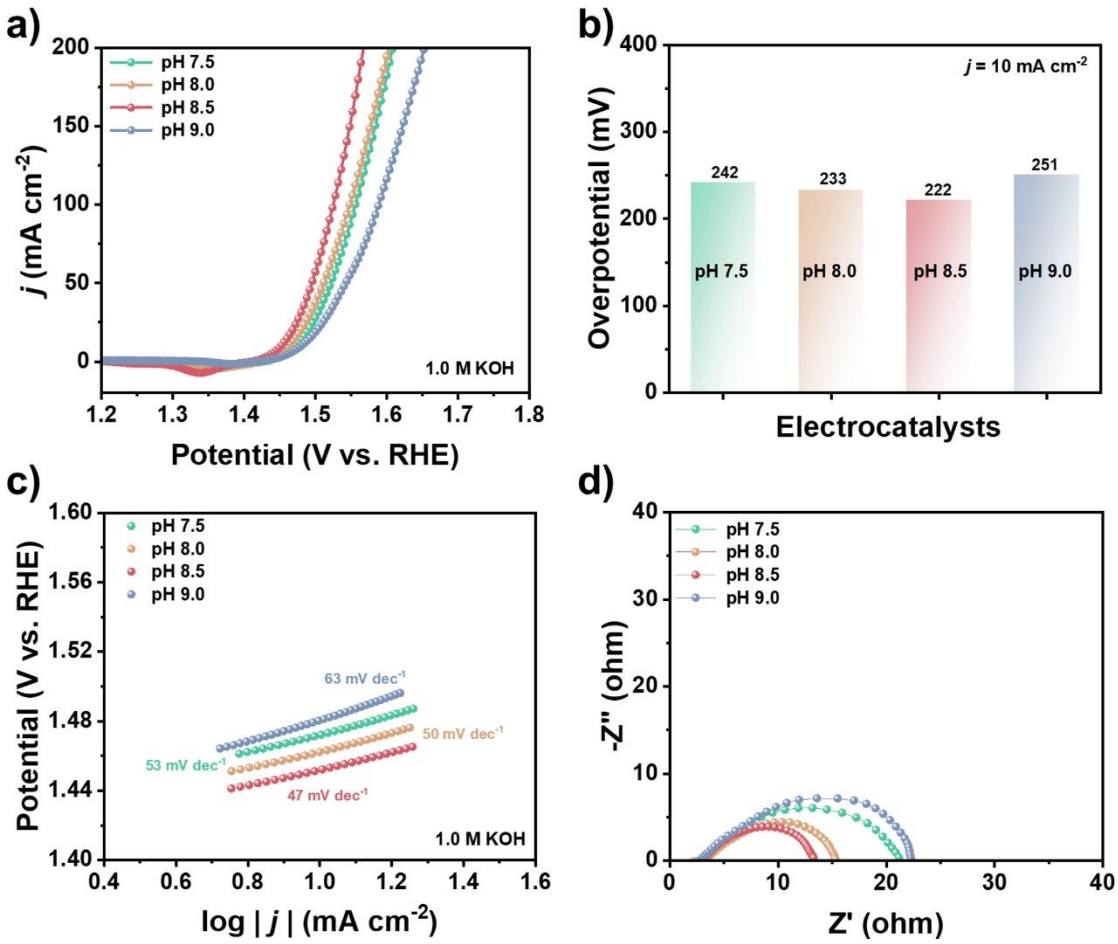

Fig. S5 (a) LSV curves of OER of NiFe hydroxide with different pH values in 1.0 M KOH. (b) Overpotentials of NiFe hydroxide with different pH values. (c) Tafel slopes of NiFe hydroxide with different pH values. (d) EIS of the NiFe hydroxide with different pH values.

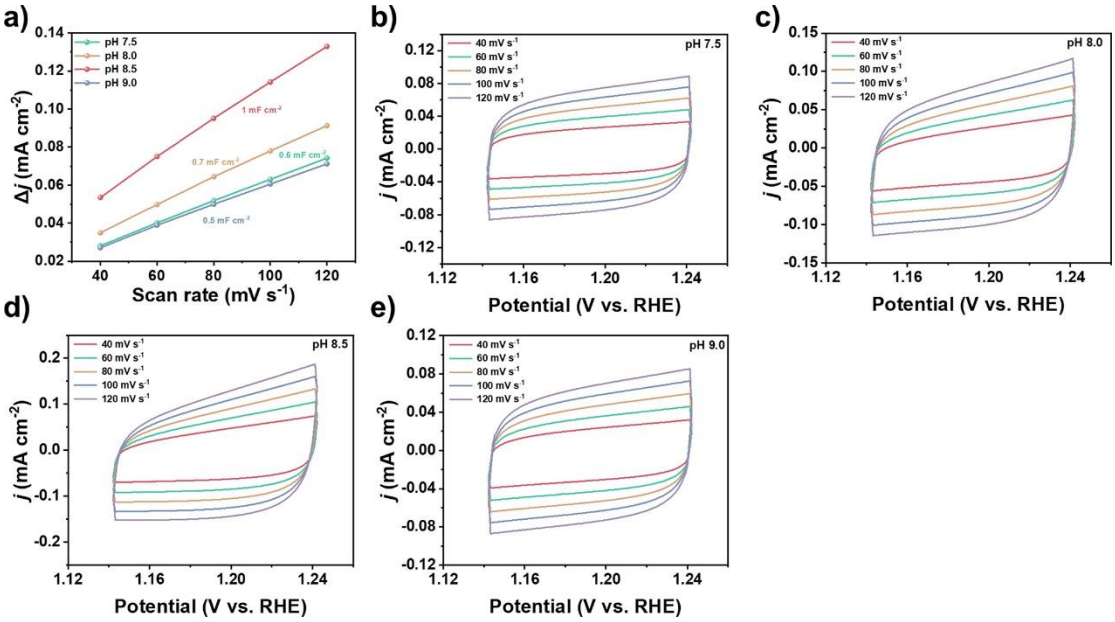

Fig. S6 (a) C_{dl} of NiFe hydroxide with different pH values. (b-e) CV curves of NiFe hydroxide with different pH values at different scan rates in 1.0 M KOH.

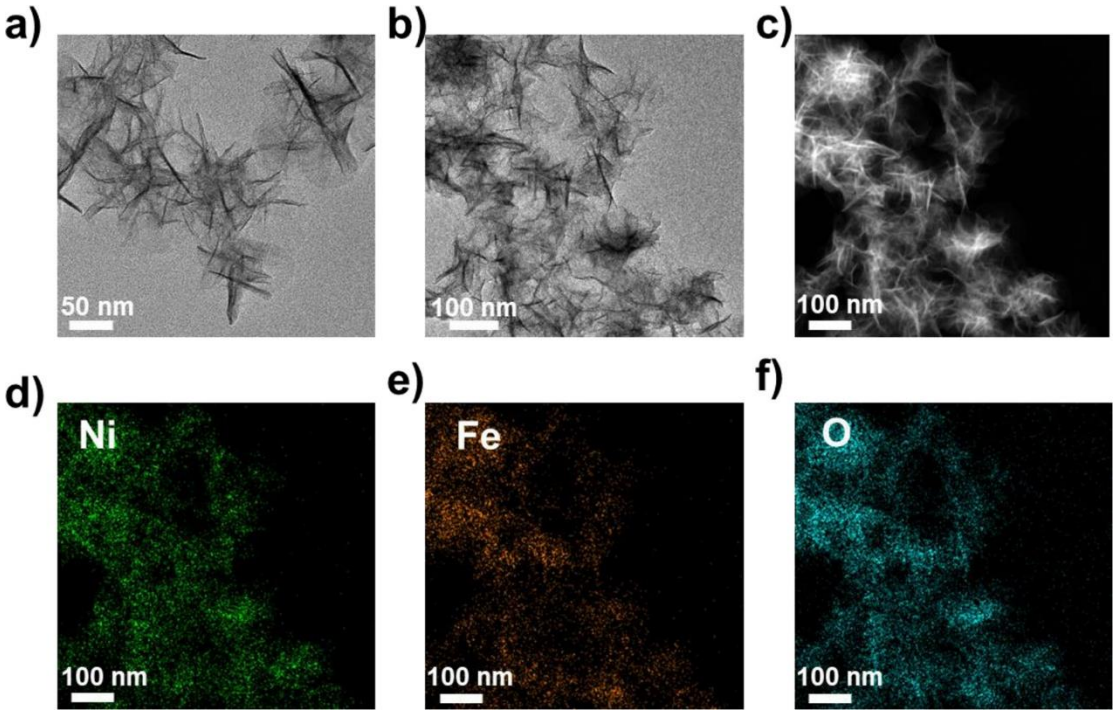

Fig. S7 Characterizations of the NiFe(III) hydroxide nanosheets. (a) TEM image. (b-d) EDS-mapping images.

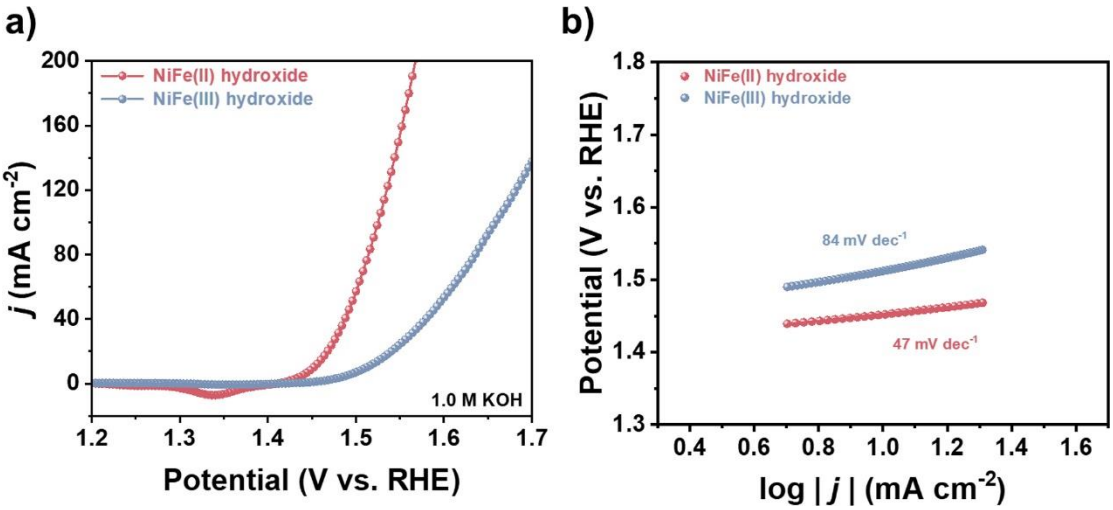

Fig. S8 (a) LSV curves of OER on NiFe(II) hydroxide and NiFe(III) hydroxide in 1.0 M KOH. (b) Tafel slopes of NiFe(II) hydroxide and NiFe(III) hydroxide.

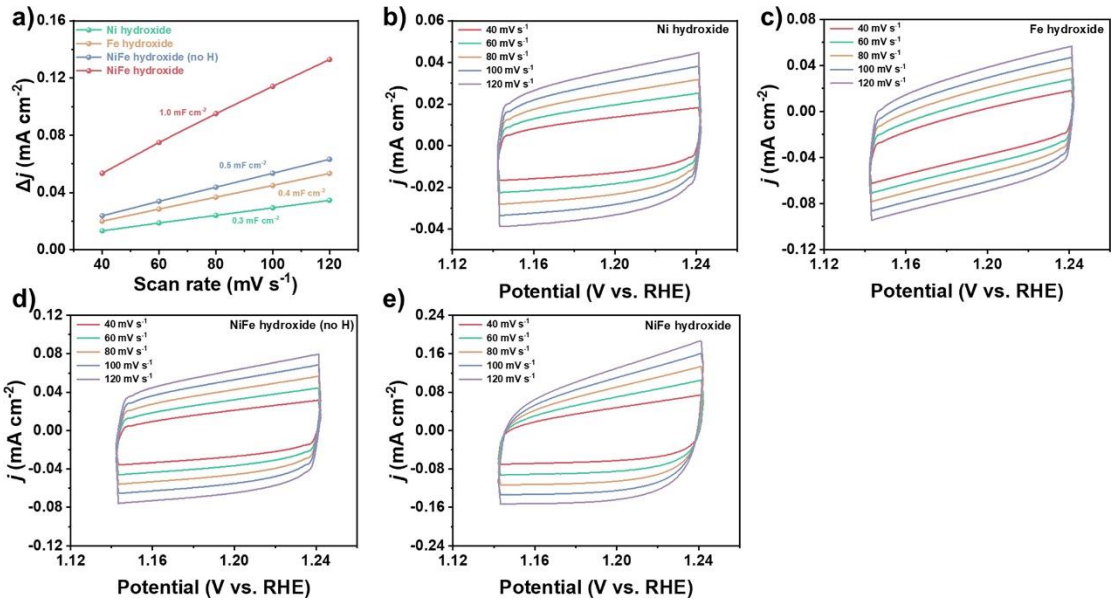

Fig. S9 (a) C_{dl} of Ni hydroxide, Fe hydroxide, NiFe hydroxide (no H), NiFe hydroxide. (b-e) CV curves of Ni hydroxide, Fe hydroxide, NiFe hydroxide (no H), NiFe hydroxide at different scan rates in 1.0 M KOH.

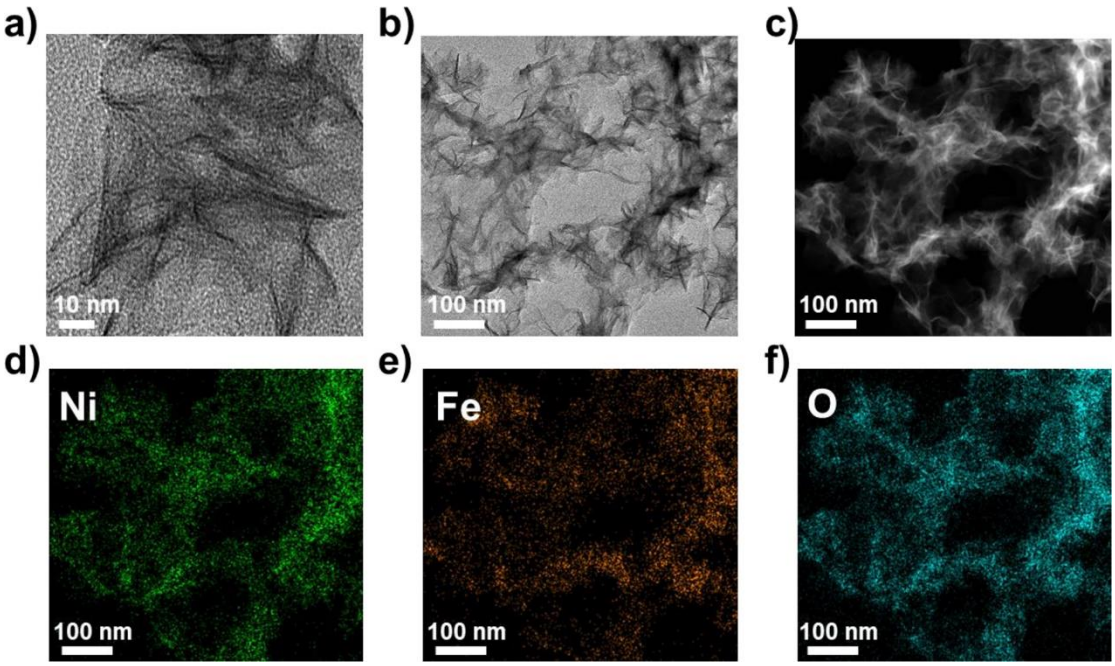

Fig. S10 TEM (a-b), EDS-mappings (c-f) of the NiFe hydroxide after OER stability test in 1.0 M KOH.

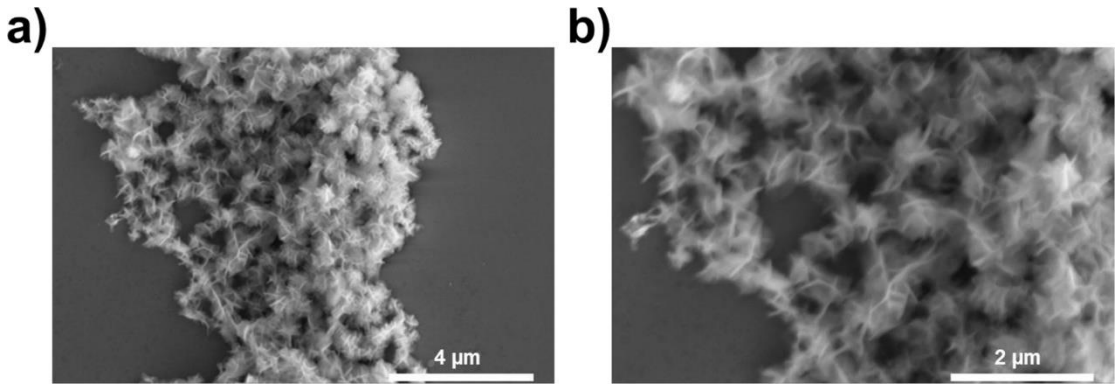

Fig. S11 SEM images of the NiFe hydroxide after OER stability test in 1.0 M KOH.

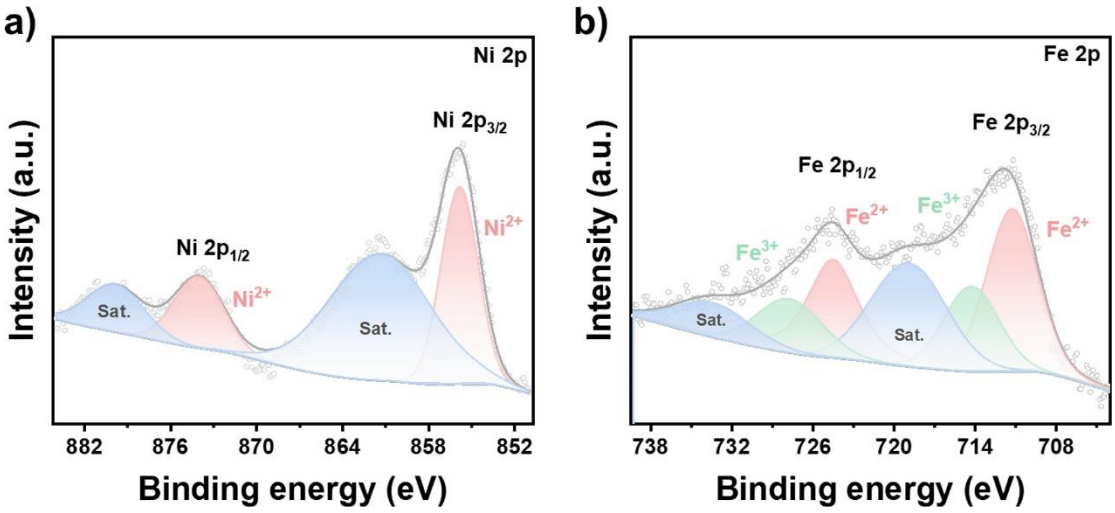

Fig. S12 Ni 2p and Fe 2p XPS of the NiFe hydroxide after OER stability test in 1.0 M KOH.

Table S1. Relative Ni and Fe percentages in NiFe hydroxide measured by ICP-OES.

Element	Percentage (%)
Ni	20.43
Fe	18.35

Table S2. Comparison of OER catalytic performances of the NiFe hydroxide catalyst and other reported catalysts in 1.0 M KOH.

Catalyst	Overpotential (η_{10}, mV)	Stability	Reference
NiFe hydroxide	**222**	**2000 h@10 mA cm^{-2}**	**This work**
Co/CoO_x@NC	307	24 h@10 mA cm^{-2}	1
NiFe MOF/NF	221	30 h@50 mA cm^{-2}	2
Pd-FeCoNiCu NPs	225	1000 h@10 mA cm^{-2}	3
CuNi	318	10 h@10 mA cm^{-2}	4
Amorphous NiFe	228	10 h@10 mA cm^{-2}	5
Ni-Co_3O_4	275	8 h@10 mA cm^{-2}	6
FeCoNiCu	294.5	25 h@10 mA cm^{-2}	7
$NiFeO_x$/Ni−V	270	25 h@10 mA cm^{-2}	8
Ag@$FeCoNiCuO_x$	249	96 h@10 mAcm^{-2}	9
FeNiCoMnRu@CNT	319	40 h@10 mA cm^{-2}	10

Table S3. Fe^{2+} percentage in NiFe hydroxide before and after OER test (measured by XPS).

	Fe^{2+} percentage (%)	**Fe^{3+} percentage (%)**
Before OER	78.06	21.94
After OER	64.84	35.16

3. References

1. Q. Zhang, K. Lian, Q. Liu, G. Qi, S. Zhang, J. Luo and X. Liu, *J. Colloid Interface Sci.*, 2023, **646**, 844-854.
2. L. Ye, M. Chen, L. Niu, Y. Gong and C. Li, *Chem. Eng. J.*, 2024, **480**, 148122.
3. X. Che, Y. Wang, L. Pan, Y. Sun, J. Zhang and H. Zhong, *Int. J. Hydrogen Energy*, 2024, **53**, 1037-1043.
4. J. Zhang, T. Quast, W. He, S. Dieckhöfer, J. R. C. Junqueira, D. Öhl, P. Wilde, D. Jambrec, Y.-T. Chen and W. Schuhmann, *Adv. Mater.*, 2022, **34**, 2109108.
5. F. Fu, Y. Zheng, N. Jiang, Y. Liu, C. Sun, A. Zhang, H. Teng, L. Sun and H. Xie, *Chem. Eng. J.*, 2022, **450**, 137776.
6. X. Li, H. Zhang, Q. Hu, W. Zhou, J. Shao, X. Jiang, C. Feng, H. Yang and C. He, *Angew. Chem. Int. Ed.*, 2023, **62**, e202300478.
7. E. Gioria, S. Li, A. Mazheika, R. Naumann d'Alnoncourt, A. Thomas and F. Rosowski, *Angew. Chem. Int. Ed.*, 2023, **62**, e202217888.
8. B. Zhu, S. Huang, O. Seo, M. Cao, D. Matsumura, H. Gu and D. Wu, *J. Am. Chem. Soc.*, 2025, **147**, 11250-11256.
9. Y. Liu, X. Li, Q. Sun, Z. Wang, W.-H. Huang, X. Guo, Z. Fan, R. Ye, Y. Zhu, C.-C. Chueh, C.-L. Chen and Z. Zhu, *Small*, 2022, **18**, 2201076.
10. C. Chen, Z. Yang, W. Liang, H. Yan, Y. Tuo, Y. Li, Y. Zhou and J. Zhang, *Journal of Energy Chemistry*, 2021, **55**, 345-354.